



Spatial Representativeness of NORS observations

Deliverable title	Spatial Representativeness of NORS observations
Deliverable number	D4.4
Revision	1
Status	Final
Planned delivery date	31/10/2013
Date of issue	01/11/2013
Nature of deliverable	Report
Lead partner	Institute of Environmental Physics, University of Bremen
Dissemination level	Public

This work has received research funding from the European Community's Seventh Framework Programme ([FP7/2007-2013]) under grant agreement n°284421.



DOCUMENT PROPERTIES

	NAME	Institute	DATE	SIGNATURE
LEAD AUTHOR	Andreas Richter	University of Bremen	01.11.2013	
CONTRIBUTING AUTHORS	Sophie Godin	CNRS		
	Laura Gomez	INTA		
	Francois Hendrick	BIRA-IASB		
	Klemens Hocke	University of Bern		
	Bavo Langerock	BIRA-IASB		
	Michel van Roozendaal	BIRA-IASB		
	Thomas Wagner	MPIC Mainz		

Table of Contents

EXECUTIVE SUMMARY	4
APPLICABLE AND REFERENCE DOCUMENTS	4
ACRONYMS AND ABBREVIATIONS	4
1. INTRODUCTION	4
2. GENERAL CONSIDERATIONS	5
2.1. Vertical resolution	5
2.2. Horizontal resolution	6
2.3. Horizontal displacement	6
3. LIDAR OBSERVATIONS	6
4. MICROWAVE OBSERVATIONS	7
5. FTIR OBSERVATIONS	7
5.1. Vertical averaging and sensitivity	8
5.2. Horizontal averaging	8
5.3. Practical implementation of FTIR averaging in NORS	9
6. DOAS ZENITH-SKY OBSERVATIONS	10
7. MAX-DOAS OBSERVATIONS	12
7.1. Mountain-top observations	13
7.2. Surface observations	14
7.3. Multi-azimuth observations	16
8. SUMMARY	18
9. REFERENCES	19

Executive summary

All remote sensing measurements average over a volume of air, and this volume can be offset from the station location both vertically and horizontally. Both the averaging and the displacement need to be taken into account when comparing columns or profiles derived from ground-based remote-sensing observations to satellite or model data. Depending on measurement technique and altitude of interest, the averaging volume and horizontal offset can vary strongly, with extreme cases of a few kilometres for lidar observations and several hundred kilometres for twilight zenith-sky observations. In this report, the relevant effects are described and characterised for all NORS remote-sensing observation techniques and methods are described that show how these effects can be taken into account in comparisons with independent data.

Applicable and reference documents

Acronyms and abbreviations

AMF	air mass factor
AOD	aerosol optical depth
AVK	averaging kernel
DAMF	differential AMF
DOAS	differential optical absorption spectroscopy
DOF	degrees of freedom of information
FTIR	Fourier transform infrared spectrometry
FOV	field of view
MAX-DOAS	multiaxis DOAS
MW	microwave radiometry
SCD	slant column density
SNR	signal to noise ratio
SZA	solar zenith angle
UV	ultraviolet
vis	visible

1. Introduction

The focus of the NORS project are ground-based remote sensing observations and their use for atmospheric characterisation, and validation of Copernicus output. In this context, the question arises what the measurement volume is for which the observations are representative, and how this can best be linked to satellite and model data which have different scales and resolutions. In this report, a short description is given on the measurement volume for which the individual observation types are representative, on the main variables influencing the measurement volume and how the latter can be estimated from the data.

In contrast to *in-situ* observations such as an ozone monitor located at the surface, remote sensing observations average over space and time providing integrated values representative for values averaged over a certain volume. When evaluating the air volume for which these measurements are representative, several levels of complexity can be envisaged:

1. The simplest question is what the air volume is over which the measurements are averaged. In this context, the relevant quantities are
 - a. Vertical resolution of the observations
 - b. Horizontal resolution of the measurements
 - c. Horizontal displacement of the measurement volume
2. A second question that can be asked is how representative the observations are for a given location. Examples are air quality stations in a city which provide very different data depending on their exact location (at the road side, in a park or in a residential area). This question becomes relevant when comparing measurements taken at high spatial resolution with satellite or model data averaging over larger areas.
3. One can go even one step further by asking for which area and volume the measurements are representative considering the history of the air masses and the atmospheric lifetime of the quantity of consideration. If measurements are integrated over a longer time period such as hours, the volume of air probed increases depending on wind speed and altitude.

In this report, the focus will be on the first question with some short discussion of the second aspect while the third point is discussed in more detail in NORS WP5.

2. General considerations

2.1. Vertical resolution

In general, all remote sensing observations use electromagnetic signals emitted from a light source. This can be

- The light scattered by a molecule or particle illuminated by a laser (lidar)
- The thermal emission of molecules in the atmosphere (microwave radiometry)
- The solar light transmitted through the atmosphere (FTIR solar or lunar absorption observations)
- The solar light transmitted through the atmosphere and scattered on molecules and particles (UV/vis DOAS)

On the way between light source and instrument, the electromagnetic signal is changed by absorption, emission and scattering, and thus some averaging of atmospheric properties between the light source and the instrument on the ground is inherent in all these observations. Depending on the technique, different properties of the signal are used to extract information for individual altitudes, namely

- The time of signal arrival (lidar)
- The line shape which depends on temperature and pressure (FTIR and MW)
- The difference in absorption signal observed under different solar zenith angles (zenith-sky DOAS at twilight)
- The difference in absorption signal observed under different elevation angles (MAX-DOAS)

These different methods provide very different vertical resolutions ranging from tens of meters for lidars to more than 10 km for zenith-sky DOAS.

2.2. Horizontal resolution

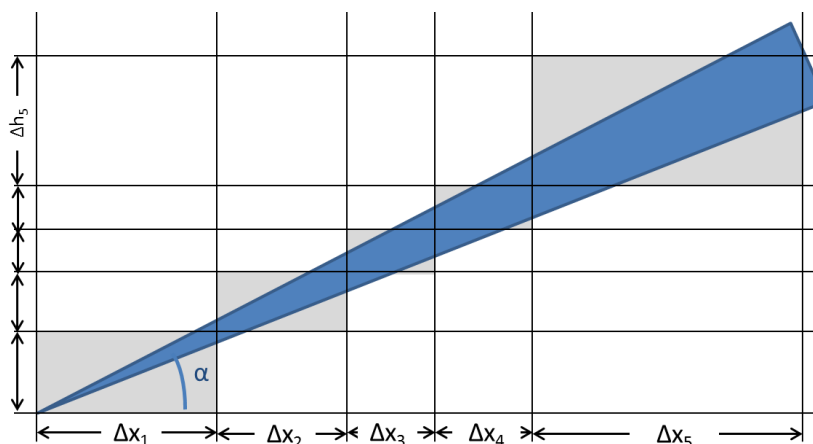


Figure 1: Sketch illustrating the dependence of horizontal averaging and displacement on accepting angle, elevation angle α , and vertical resolution Δh .

With the exception of multi-azimuth MAX-DOAS, none of the NORS measurement techniques is designed to provide horizontally resolved information. However, the observations are not limited to a narrow slab of air located vertically above the instrument but rather average over a volume of air having a certain horizontal extent, usually increasing with altitude. The amount of horizontal averaging depends on the acceptance angle of the instrument, the elevation angle of the measurements, the altitude, the vertical resolution, and in the case of DOAS observations also on the state of the atmosphere. This is illustrated in the sketch in Figure 1 for a simplified situation. In reality, the situation is complicated by the horizontal and vertical smoothing performed in the retrieval.

2.3. Horizontal displacement

As already shown in Figure 1, the horizontal displacement of the air volume probed is linked to the elevation angle and altitude. While this is true for all measurement techniques, additional horizontal displacement needs to be taken into account for DOAS observations, where the light path can in first approximation be seen as consisting of two parts, one from the sun to the scattering point and a second one from the scattering point to the instrument. Depending on solar position, this can lead to very large displacements in the stratosphere.

3. Lidar observations

Arguably the simplest situation with respect to spatial representativeness is found for lidar observations. Here, the situation is very similar to that shown in Figure 1, and with an orientation to the zenith, the horizontal displacement is minimal. The vertical resolution is very good and horizontal averaging determined by the size of the laser beam and the acceptance angle of the telescope. Therefore, the horizontal averaging increases with altitude. As lidar measurements are often integrated over long time periods, the effective volume of air over which the measurements are integrated is dominated by horizontal wind speed and thus current meteorological conditions. For a typical ozone profile measurement in the 20 - 50 km altitude range, lidar signals are averaged over about 4 hours, which results in a horizontal resolution of 100 km to 200 km for the retrieved ozone profile.

4. Microwave observations

For microwave observations, the horizontal displacement is determined by the geometry of the accepting angle of the antenna and the elevation angle of the measurements (Figure 2). The latter is determined by considerations of signal to noise, main altitude of interest and atmospheric opacity. The accepting angle is about 2 degrees for ozone microwave radiometers at 110 or 142 GHz (Parrish, 1994). As the vertical resolution of microwave retrievals is relatively low, the horizontal extent over which the volume is averaged can become quite large at small elevation angles. While the ozone radiometer at Ny-Ålesund has an elevation angle of 20 degrees, the ozone radiometer at Bern has an elevation angle of 40 degrees due to the higher amount of tropospheric water vapour.

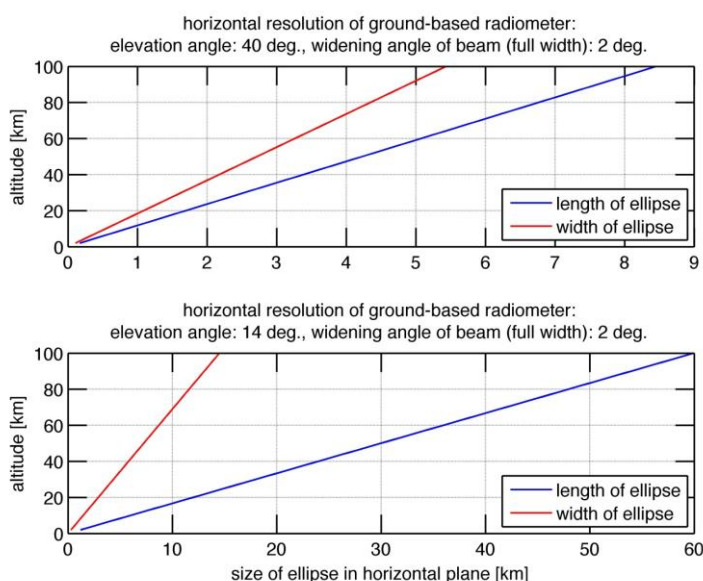


Figure 2: Main axis of the ellipse formed by the projection of the beam cross-area of a microwave radiometer on the surface as a function of altitude. A widening angle of 2° was assumed and data are shown for two elevation angles, 40° (top) and 14° (bottom).

5. FTIR observations

For FTIR observations, the averaging volume is determined by the light path between the instrument and the sun in combination with the vertical resolution. As the angle under which the sun disk appears on the surface is relatively small (0.5°), the widening of the beam between the instrument and the top of atmosphere is relatively small. However, the observational line follows the sun, and therefore both the elevation angle and the azimuth of the observations change over the course of the day. This results in larger averaging volumes at low sun than around noon and in a systematic change of horizontal displacement over the day and the seasons. For large solar zenith angles, the curvature of the earth needs to be taken into account.

5.1. Vertical averaging and sensitivity

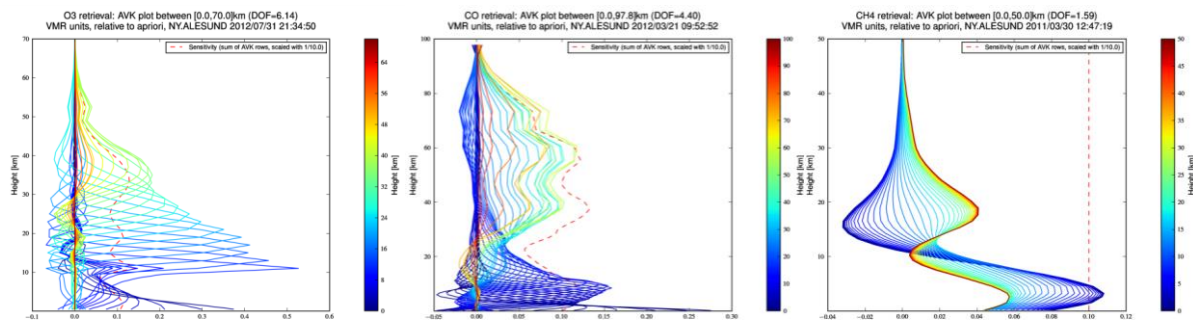


Figure 3: Example of averaging kernels for measurements of O₃ (left), CO (middle), and CH₄ (right) for Ny-Ålesund. The vertical resolution for the three products is quite different, resulting in varying degrees of spatial averaging. The coloured curves in the plots are the rows of the AVK matrix where each element in the row is plotted against the corresponding grid height. Each curve or row of the AVK is colour coded according to the height of the corresponding row index (see horizontal lines). The sensitivity curve (dashed red) represents the fractional sensitivity of the retrieved profile at each altitude to the measurement.

For each NORS FTIR target product (O₃, CO and CH₄) at each NORS site, a typical vertical averaging kernel and sensitivity curve is determined (red dashed line in Figure 3). The averaging kernels depend on the measurement characteristics (e.g. SNR, spectral resolution, and SZA), and on the inversion method parameters (optimal estimation or Tikhonov). Sensitivity curves are only meaningful when the retrieval method used is optimal estimation. Indeed, for Tikhonov regularization, one can show that the sensitivity is constant and equal to one.

For FTIR measurements, sensitivity typically lies between the surface and 60 km. CO retrievals may show an increased sensitivity in the upper stratosphere (e.g. at Ny-Ålesund). The averaging kernels do not take into account the effects of horizontal averaging and displacement or any horizontal variations in atmospheric parameters.

As shown in Figure 3, the vertical resolution depends strongly on the species of interest. Therefore, the horizontal averaging for ozone (> 6 DOF) is much smaller than that for CH₄ (DOF = 1.5). As vertical resolution also varies between instruments, and with latitude, seasons and time of the day, the averaging has to be computed for each individual measurement.

5.2. Horizontal averaging

The vertical profiles retrieved from FTIR observations are based on an optimal estimation inversion using a-priori data to constrain the otherwise ill-posed problem. Ideally, the inversion method would take into account the fact that depending on altitude, the measurement point is offset from the instruments site: instead of taking a single vertical a-priori profile, the method would require a 3D (latitude/longitude/altitude) gridded a-priori field of target and interfering gas concentrations plus an a-priori temperature/pressure 3D field, and use the line of sight at the time of measurement and the FOV of the instrument to get a spatial volume in which the target gas has absorbed the measured light.

In this case the retrieval method would produce gridded data and the corresponding AVK is a tensorial object that works on 3D gridded data instead of vertical profiles. Such an extended AVK provides for each retrieval grid point a 3D gridded set of coefficients weighing the true and a-priori gridpoints. Similar to the vertical AVK, the weighing coefficients should be

approximately one for the gridpoints in the neighborhood of each retrieved grid point along the line of sight and vanish for distant grid points. Sensitivity is centered around the line of sight. Horizontal averaging describes this kind of extended AVK, i.e. taking into account the geographical off-location and corresponding sensitivity from the measurement site.

In practice, the inversion software SFIT-2 provides vertical averaging kernels, but it cannot provide horizontal kernels because it assumes a horizontally homogeneous atmosphere and because its radiative transfer calculations account only for the vertical gradients.

To describe the horizontal averaging of FTIR measurements, we use an off-line C++ routine, called Raytrace [BIRA-IASB, Raytrace], which determines the path through the atmosphere of the captured light during the measurement.

5.3. Practical implementation of FTIR averaging in NORS

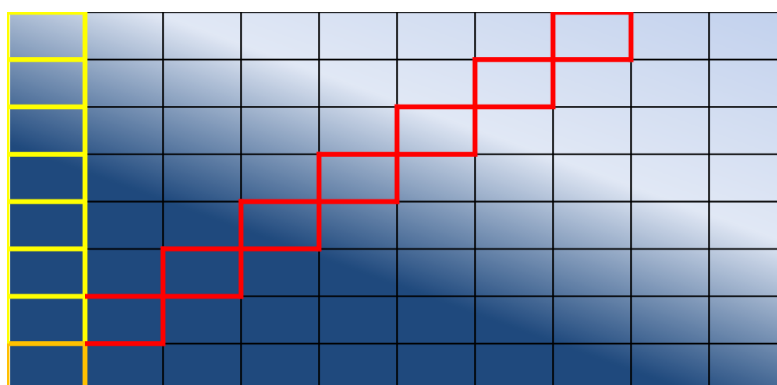


Figure 4: sketch illustrating the difference between taking the vertical profile above the station (yellow boxes) and the vertical profile along the light path (red boxes) in the presence of an atmospheric gradient (blue shading). In this case, the vertical profile encountered along the light path is much steeper than the one above the instrument.

To compare retrieved FTIR data against gridded (model) data, a profile is model grid along the line of sight (see

Figure 4). The Raytrace tool allows to generate the latitude and longitude angles along the line of sight for any given altitude. Using basic interpolation techniques (i.e., a bilinear interpolation on the latitude and longitude), the tool allows to extract a profile defined on the vertical grid of the measurement. This profile can then be smoothed with the appropriate vertical averaging kernel.

The horizontal averaging technique outlined above and employed in the NORS validation server is an approximation of using the true gridded AVK. The technique accepts gridded data (in the case of NORS, the gridded MACC-II products) from which a vertical gas concentration profile is extracted along the line of sight determined from the Raytrace tool, using basic interpolation techniques. This profile can then be smoothed along the altitude dimension with the appropriate vertical averaging kernel. This technique implies that we approximate the true gridded AVK with an AVK whose only non-vanishing weighing coefficients are limited to the gridpoints along the line of sight and equal the components of the vertical AVK.

6. DOAS zenith-sky observations

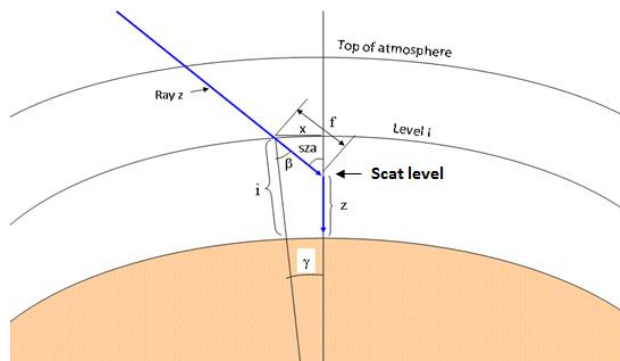


Figure 5: Sketch of the light path for zenith-sky observations. Indicated is the distance x that the measurement point has at altitude level I for a scattering altitude z at solar zenith angle SZA .

For zenith-sky observations, the horizontal displacement of the measurement volume depends mainly on solar zenith angle (sza). In contrast to the FTIR measurements, the light path has in first approximation two separate parts – one from the sun to the scattering point in altitude z which is determined by the solar position, and a second one passing vertically through the atmosphere from altitude z to the instrument on the ground (Figure 5). The horizontal displacement x from the instrument location can be computed for each scattering height z by

$$x(z, i) = (i - z) \cdot \tan(sza)$$

For the effective signal, the average over the horizontal displacements for all scattering altitudes z needs to be calculated, weighted by the respective radiation received from this altitude at the surface $WF(z)$:

$$d(i) = \frac{\sum_{z, i=0}^{top-atmosphere} x(z, i) * WF(z)}{\sum_{z, i=0}^{top-atmosphere} WF(z)}$$

The resulting distances d are shown in Figure 6, left panel and can be as large as 500 km in the stratosphere at twilight. In the right panel of Figure 6, the resulting 2d averaging kernel is shown, illustrating both, the vertical smoothing and the horizontal displacement. The display is oriented towards the sun and basically shows a slice through the real 3d averaging kernel which has little extent orthogonal to this plain but moves over the day with the solar azimuth. As the distances can become large at higher altitudes and low sun, the curvature of the atmosphere needs to be taken into account which leads to a change in SZA along the light path. In case of a photolytically active species such as NO_2 , this complicates interpretation of the results and a photochemical correction is needed during twilight.

So far, the discussion assumed that the retrieved quantity is computed from a single measurement. If several observations at different SZAs are combined to retrieve a vertical profile, it is not at all straightforward how to compute the horizontal displacement for the resulting profile. As a very first approximation, one could assume that each measurement mainly contributes to the retrieved concentration in one altitude which would then have the

horizontal displacement characteristic for this solar zenith angle. However, no formal treatment of this problem has been performed so far.

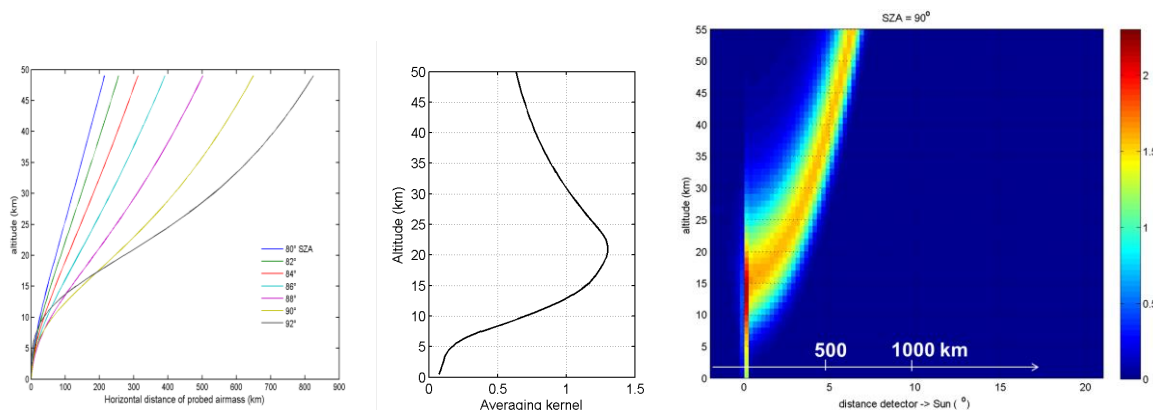


Figure 6: Horizontal displacement in zenith-sky DOAS observations. Left: Average displacement of the measurement point for different altitudes at different solar zenith angles. Middle: 1D averaging kernel at 90° SZA. Right: 2d averaging kernel at 90° SZA, combining the effect of horizontal displacement and vertical smoothing.

In twilight measurements under atmospheric conditions having large gradients in the concentration field of the quantity of interest, taking the effective measurement location into account is of importance in the use of ground-based zenith-sky data for satellite or model validation. This is illustrated in Figure 7 where the change of effective measurement location in Marambio is shown (left) and related to the stratospheric NO_2 field as observed by satellite (right).

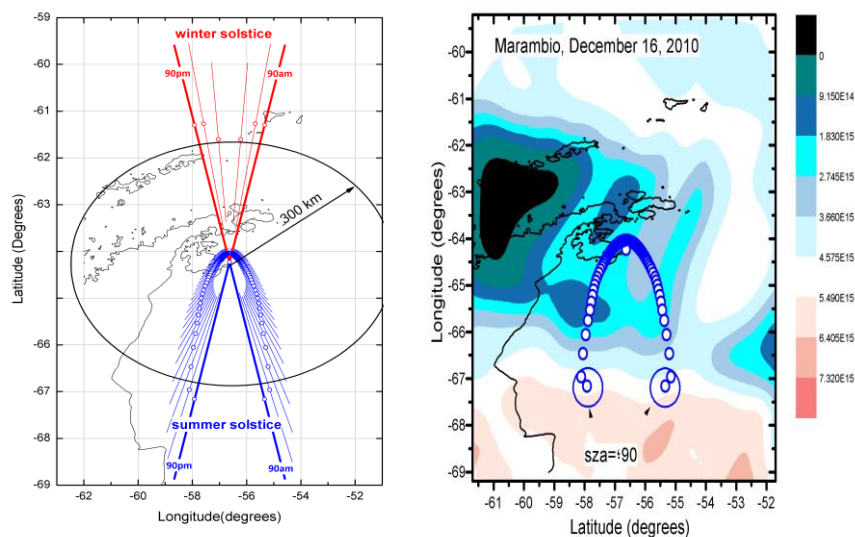


Figure 7: Effective measurement location of zenith-sky measurements in Marambio. Left: at winter (red) and summer (blue) solstice. The strong line is for 90° SZA. Right: for December 16, plotted over the NO_2 distribution to illustrate the importance of proper assignment of measurement location.

7. MAX-DOAS observations

For measurements in the troposphere, the telescope of DOAS instruments is pointed towards the horizon, thus strongly increasing the sensitivity towards absorptions in the lowest atmospheric layers. By taking observations at different elevation angles, some vertical information can be retrieved from the variation in observed absorption, usually with 1.5 – 3 DOF. By analysing the signal of the O_2 dimer O_4 , information on the aerosol distribution can also be retrieved (usually AOD and vertical distribution) as the vertical profile of O_4 is well known. This aerosol information is also needed for the inversion of vertical constituent profiles.

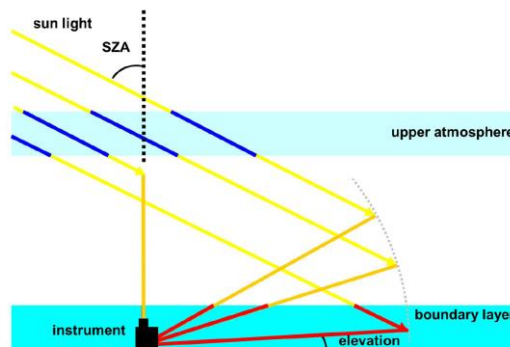


Figure 8: Simplified light path for MAX-DOAS observations. The light path length in the boundary layer depends mainly on elevation angle and only weakly on the solar position while for the upper atmosphere, the light path depends mainly on solar zenith angle and is the same for all viewing directions including zenith-sky.

Compared to zenith-sky observations, the characterisation of horizontal representativity is further complicated. While in single scattering approximation the light path can still be divided into two parts, the first being determined by the solar position, the second part from the scattering point to the instrument depends on the viewing azimuth and elevation of the instrument (Figure 8). Also, the distance of the last scattering point from the instrument is strongly dependent on wavelength and aerosol load and profile and can only be determined from the measurements themselves using the O_4 absorption. This is illustrated in Figure 9, where 2d box air mass factors (box-AMF) are shown for two wavelengths without aerosols (left and middle) and with an AOD of 0.5 in the lowest 1 km. Without aerosol, horizontal displacements of up to 200 km are possible at 500 nm, of about 50 km at 360 nm and much less in the presence of aerosols.

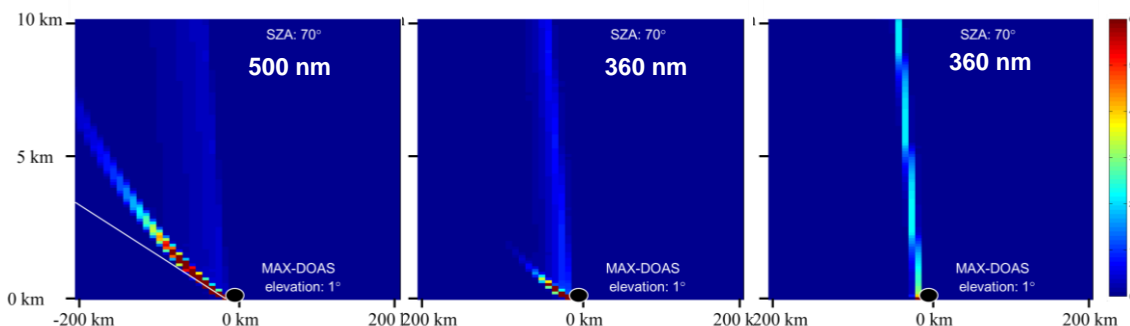


Figure 9: 2d box AMF for MAX-DOAS observations at 1° elevation and an SZA of 70°. Left: 500 nm, no aerosol. Middle: 360 nm, no aerosol. Right: 360 nm, AOD 0.5 in lowest km. All calculations have been done using a horizontal

grid of $8 \times 8 \text{ km}^2$ and a vertical grid of 100 m. The deviation of the line of high box-AMF from a straight line is caused by the Earth's curvature.

7.1. Mountain-top observations

For MAX-DOAS observations from a mountain station in the free troposphere, observations at 0° elevation angle can reach very long distances as there are no obstructions and the aerosol load is usually low. In this case, the effective light path length and thus the horizontal averaging can be well estimated using the O_4 absorption in the measurement in combination with the O_4 concentration at the altitude of measurement:

$$d = \frac{SCD_{\text{O}_4}(\alpha=0^\circ, SZA_1, t_1) - SCD_{\text{O}_4}(\alpha=90^\circ, SZA_2, t_2)f}{[\text{O}_4]_{\text{station}}}$$

Here, α is the elevation angle, SCD is the slant column density and f is a factor correcting for the change in air mass factor between the two measurements at SZA_1 and SZA_2 . The assumption behind this formula is that the scattering point in zenith-sky direction is close to the instrument and thus the light path above the horizontal layer is similar between the 0° and 90° elevation measurements. If the 90° direction cannot be used for some reasons, another high elevation measurement such as 70° can also be used. The direction of the averaging is determined by the pointing of the telescope, the averaging across the viewing direction depends on the FOV of the instrument which is usually small ($< 1^\circ$).

In Figure 10, the horizontal light path length as determined from the O_4 signal is shown for observations in Izaña. Clearly, the light path is long in the absence of aerosols and reduced when desert dust is transported to the observation altitude.

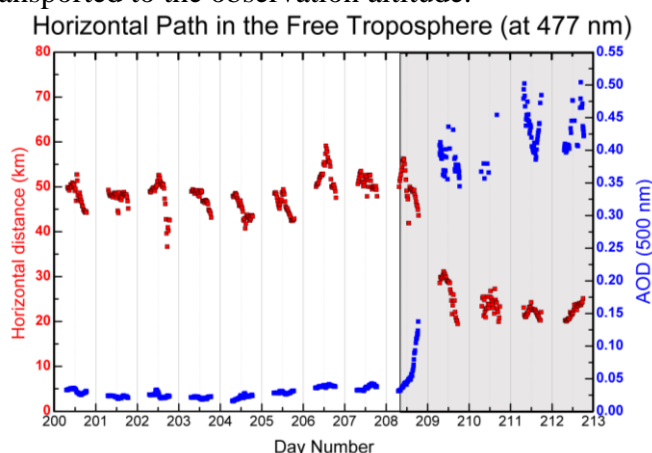


Figure 10: Light path length estimated from the O_4 signal for measurements in Izaña in comparison to AOD. At low AOD, path lengths of 50 km are obtained while for an AOD of 0.45, the horizontal path is only 20 km.

In Izaña, the measurements are rarely affected by clouds as the station is usually above the cloud deck. In other stations such as Jungfraujoch, clouds in the field of view can strongly reduce the horizontal light path, and in cases where the station is within the clouds, the difference in signal between the horizontal and zenith direction can vanish completely (Figure 11).

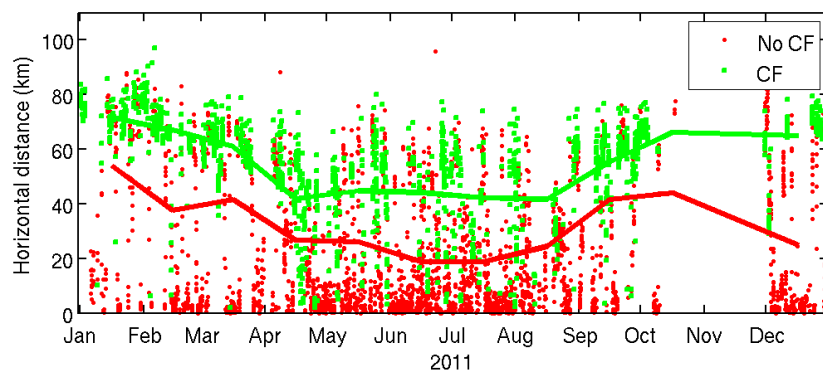


Figure 11: Horizontal light paths determined from O_4 observations at the Jungfraujoch station. Data taken under cloud free conditions (green) have systematically longer light paths. As the Jungfraujoch station is higher than Izaña, scattering is reduced and the horizontal light path is longer.

If the same approach is applied to observations in a polluted environment such as Athens, the horizontal light path lengths are expected to be shorter. As shown in Figure 12, this is indeed the case for observations from Penteli hill (500 m altitude). On most days, light paths in the less polluted directions are slightly longer than towards the city, but differences are relatively small and values range between 20 and 30 km on most days. One of the viewing directions is pointing towards a mountain located at 17.5 km distance and this is reflected in a lower retrieved horizontal path length.

As a result of the higher air density and the presence of aerosols, multiple scattering cannot be ignored for the Athens measurements and the real geometry might not be well described by the simple model used for the calculations. Also, as at Jungfraujoch, clouds can have a strong impact on the light path and thus the horizontal averaging.

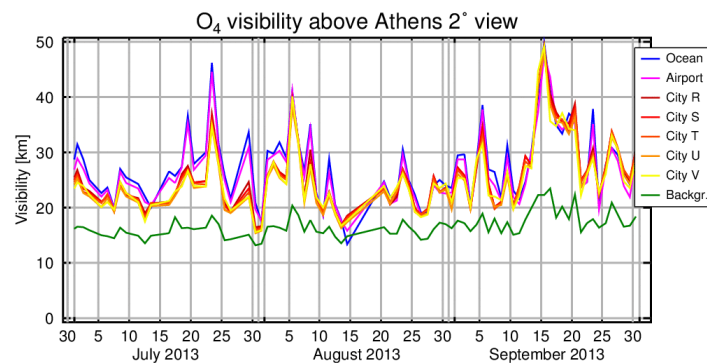


Figure 12: Horizontal light path determined from the 2° elevation angle O_4 columns retrieved from Penteli hill, Athens. The viewing directions “ocean” and “airport” are usually less polluted than the “city” observations and thus have slightly larger light paths. The “background” direction is pointing at a mountain in 17.5 km distance and thus has limited free range.

7.2. Surface observations

For MAX-DOAS measurements at the surface, the horizontal averaging for elevation angles other than the 0° value used above in the discussion of mountain top observations is of interest. In that case, it is also interesting to investigate the change of horizontal displacement and averaging with altitude. This is illustrated in Figure 13 for different elevation angles.

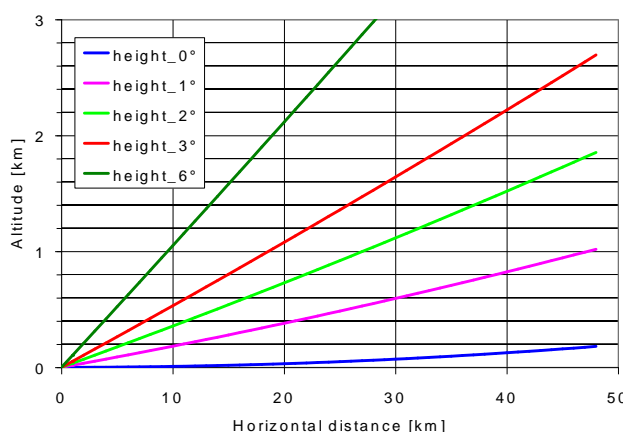


Figure 13: Relationships between altitude and horizontal distance of an air mass observed by MAX-DOAS observations for different elevation angles. The effect of the earth's curvature is taken into account

The light path length of MAX-DOAS observations is usually derived from the O_4 columns. It depends strongly on aerosol load as illustrated in Figure 14 for an elevation of 1° at 360 nm. From the figure it is also clear that at lower AOD, the measurements are more sensitive to higher altitudes (as the light path becomes longer and distance and altitude are linked, see Figure 13).

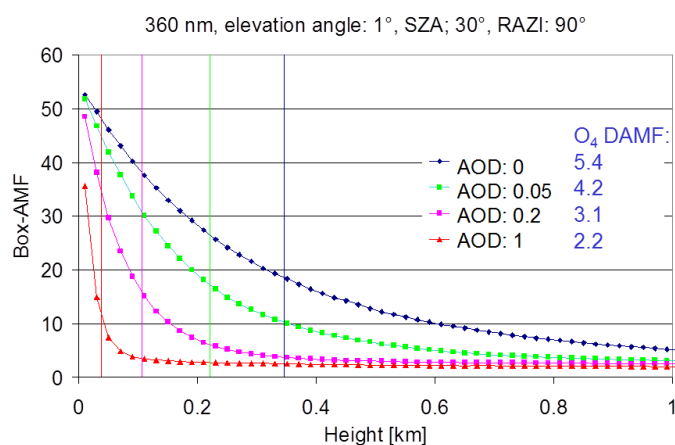


Figure 14: Change of box-AMF with altitude for different aerosol scenarios at 360 nm, an elevation angle of 1° and 30° SZA.

In principle, the link between O_4 absorption and horizontal sensitivity range (defined as the distance at which the DAMF decreases to $1/e$ of its value at the location of the instrument within 60 m distance) depends on many parameters including wavelength, elevation angle and aerosol profile. However, by evaluating a large range of situations with a radiative transfer model, a rather compact relation is found between the two quantities which can be approximated by a low order polynomial as illustrated in Figure 15. From these tabulated polynomials, the horizontal extent of the MAX-DOAS averaging volume can be estimated based on the O_4 column retrieved from the same measurements.

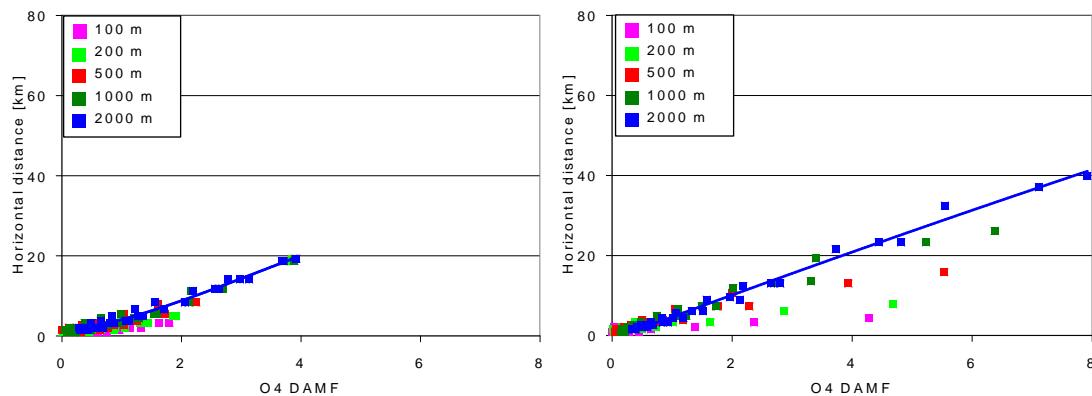


Figure 15: Relationships between the retrieved O₄ differential AMF (1° elevation – 90° elevation) and the horizontal sensitivity range for 1° elevation angle and 360 nm (left) and 630 nm (right). (SZA: 60°; relative azimuth angles: 0°, 90°, 180°). The different colours represent results for different aerosol extinction (box) profiles

As already briefly discussed for zenith-sky observations, estimation of averaging volumes and horizontal displacement becomes even more complex if not applied to columns retrieved from one measurement but to profiles retrieved from a series of observations, here in different viewing directions. As each viewing direction has its own horizontal displacement and averaging, the corresponding values for the profile may depend in a complex way on altitude but also on the a priori profile used and the DOF of the specific retrieval. As a first approximation it might be useful to take a low elevation observation (elevation angle $\leq 3^\circ$), evaluate the horizontal averaging for the AOD derived from the O₄ absorption and take this as an upper limit for the horizontal averaging of the whole profile. If the horizontal sensitivity range should be provided as function of altitude, the height-distance relationship shown in Fig. 13 might be used. More sophisticated estimates might become available in the future based on retrievals using 3d Monte Carlo radiative transfer models with 3d averaging kernels and a priori profiles (see also discussion in the FTIR section).

7.3. Multi-azimuth observations

Some MAX-DOAS instruments have the ability to point in different azimuth directions in addition to varying the elevation angle. These measurements can be used to get an insight into the horizontal variability of the absorber fields at the scales of the horizontal path length of these instruments which are of the order of 5 – 20 km. With this additional information a better understanding can be gained of how representative the observations are for a larger area around the measurement station, important information for comparisons with satellite or model data.

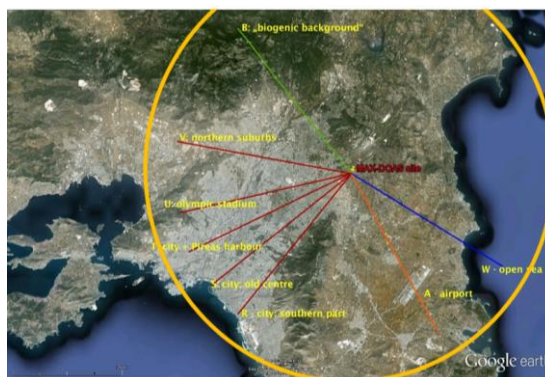


Figure 16: Observation geometry for the MAX-DOAS measurements in Athens. The city is to the left of the instrument, the blue, orange and green directions point at less polluted areas. The yellow circle indicates the 20 km range (compare Figure 12).

The MAX-DOAS instrument on Penteli hill in Athens has the required ability to change the azimuthal viewing direction and from its observation point at the margin of the city covers both the main city and less polluted regions (see Figure 16). Typical horizontal path lengths of this instrument have been shown in Figure 12 indicating that usually the city is fully covered, in agreement with visual impression when looking at the city from the station. It should be noted that from the elevated observing point (500 m) the view is not obstructed towards the city but in case of a shallow boundary layer might not be representative for concentrations at the surface.

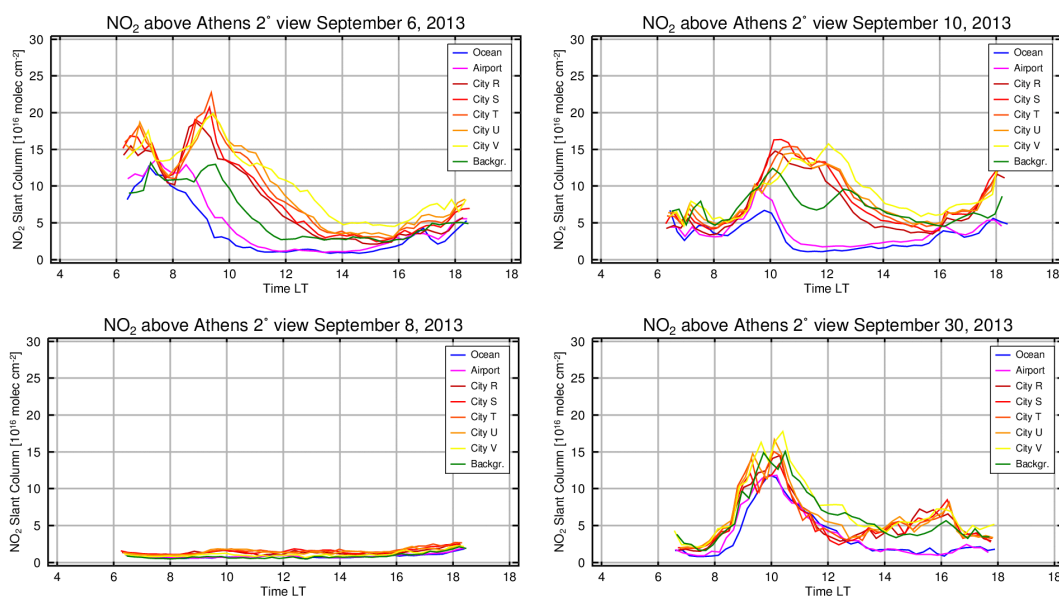


Figure 17: Four days of measurements in Athens during September 2013 demonstrating the variability of NO₂ levels and the respective horizontal gradients. On some days, the background directions show much lower NO₂ values than the city directions at least part of the day while on other days, all directions behave similar. On September 6, large spatial gradients are seen also within the city, probably linked to transport of polluted air masses.

On many days, large gradients are observed in NO₂ observations in different directions (Figure 17). This is linked to the distribution of emissions which are highest in the city and harbour regions and lowest in the ocean direction. Over the day, pollution is transported

towards the mountains or the sea depending on wind direction, leading to distinct and highly variable diurnal patterns and gradients. When looking at the relative RMS of the NO_2 column observed in the different regions, values between 0.1 and 0.7 are found on most days. This variability is determined by both, variations in light path and in NO_2 . However, division by the O_4 column to remove the light path effect does not reduce the RMS much, indicating that the RMS is dominated by NO_2 gradients. This is in contrast to the situation for H_2O which has a lower RMS to start with which is further reduced by a factor of 2 when applying the O_4 correction.

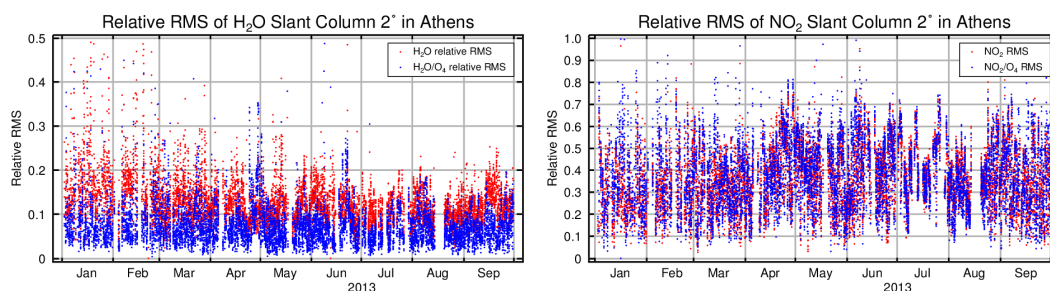


Figure 18: Variability of H_2O (left) and NO_2 (right) with (blue) and without (red) correction of the light path length by dividing with the O_4 column. Only values taken at $\text{SZA} < 70^\circ$ are shown. Note the difference in scales.

8. Summary

All remote sensing observations average over a measurement volume, and the data retrieved from the measurements are representative for a certain air volume. This air volume is not necessarily located above the measurement location, and the horizontal displacement of the air volume for which the measurement is representative depends on altitude.

For lidar and microwave radiometer observations, determination of the averaging volume is relatively simple and the horizontal displacement depends mainly on instrument pointing. For FTIR solar or lunar occultation measurements, the instrument tracks the sun or moon, and horizontal displacement thus varies depending on the position of the sun or moon. For zenith-sky DOAS observations, the averaging volume is also displaced towards the sun, and in twilight measurements, this displacement can become several hundred kilometres. For MAX-DOAS observations, the horizontal averaging volume depends strongly on aerosol loading, wavelength and viewing direction and varies between a few km in the polluted BL and up to 80 km from the top of a mountain under clean conditions.

Representation of horizontal averaging and displacement can be implemented in a relatively simple way for lidar, microwave and FTIR observations. For DOAS zenith-sky observations, the implementation is also straightforward for column measurements but not so obvious for profile retrievals. For horizontal observations for example from mountain tops the horizontal averaging can also be well described for MAX-DOAS instruments. For surface observations in particular under high aerosol conditions more statistical approaches need to be taken and for profile retrievals from multiple viewing directions, no quantitative treatment is possible yet.

From MAX-DOAS measurements using multiple azimuthal observation directions, the horizontal variability of the atmospheric absorber fields can be estimated on distances of several tens of kilometres, and as expected, they can be large in the vicinity of sources such as large cities.

9. References

- L. Gomez, M. Navarro-Comas, O. Puentedura, Y. Gonzalez, E. Cuevas, and M. Gil-Ojeda
Atmos. Meas. Tech. Discuss., 6, 8235-8267, 2013
- Parrish, A., "Millimeter-wave remote sensing of ozone and trace constituents in the stratosphere," Proceedings of the IEEE , vol.82, no.12, pp.1915,1929, Dec 1994, doi: 10.1109/5.338079
- Raytrace, BIRA-IASB, a C++ tool to compute the path of solar light through the atmosphere.